Consistent boundary element method for crack propagation problems

Guilherme O. Rabelo[1], Luiz C. Wrobel[1], Ney A. Dumont[1]

[1]*Dept. of Civil and Environmental Engineering, Pontifical Catholic University of Rio de Janeiro*
R. Marquês de São Vicente, 225 - Gávea, 22541-041, Rio de Janeiro, Brasil
guilhermeorabelo@gmail.com, luiz.wrobel@puc-rio.br, dumont@puc-rio.br

Abstract. *This paper presents the development of a crack propagation code to be implemented in a computer program based on the consistent boundary element method. This method has as its main characteristic an exact resolution of singularity problems inherent to the formulation. Furthermore, with this method, it is possible to represent the crack geometry of the models with openings in the micrometer range, similar to the cracks presented in laboratory tests. In this study, two models with different geometries are analyzed, using the same load, in order to represent pure mode I and mixed mode (modes I and II) loading configurations. The performance of this method is compared with the results of other papers found in the literature. As a crack propagation criterion, the maximum stress in the proximity of the crack tip and the stress intensity factor obtained through the crack tip opening displacement are analyzed. A study was also carried out on the propagation angle and crack stability, aiming at improving the accuracy of the model results and reducing the computational cost of the simulations. The study presented in this article is a work in progress.*

Keywords: Consistent boundary element method, fracture mechanics, crack propagation,

1 Introduction

Numerical models applied to engineering problems have gained extreme importance in the academic and professional spheres, becoming practically mandatory in some sectors of science. Computational development and the use of various mathematical techniques allow for the analysis of problems with precision, often obtained through the study of differential or integral equations.

The boundary element method is a numerical technique that has wide application and presents extremely reliable results, using integral equations, presenting a reduction in the difficulty of modeling and computational effort due to the mesh discretization being located only in the region of the contour or surface of the studied object, reducing the system of equations utilized.

For fracture propagation problems, the method is ideal as it is possible to extend the mesh along the propagation path without the need for major changes in the overall mesh processing, simply by adding new elements to the new structure configuration.

The objective of this work is to apply the boundary elements method using a consistent formulation developed by Dumont [1, 2], which solves existing singularity problems in the formulation of the conventional method, as well as improvements in the interpolation process of surface forces. The entire code was developed in Maple [3].

2 The consistent boundary element method and fracture mechanics

2.1 Consistent formulation of the boundary element method

The formulation of the boundary element method for elasticity problems can be found in several ways [1][4], from the development of the stress field equation that satisfies equilibrium in the domain:

$$\sigma_{ji,j} + b_i = 0 \tag{1}$$

in such a way that, through the use of concepts and properties of the theory of elasticity, it is possible to find the fundamental equation of the boundary element method, presented in its matrix form:

$$\mathrm{Hd} = \mathrm{Gt} + \mathrm{b} + \varepsilon \tag{2}$$

The matrix H is a kinematic transformation matrix that transforms displacements between two reference systems, G is a flexibility-type matrix, b is a vector of nodal displacements equivalent to the field forces applied in the system and ε is an error, the magnitude of which is defined by the mesh refinement, which affects the accuracy of the balance between surface forces and body forces, and the amount of rigid body displacements u_{is}^{r}, implicit in the fundamental solution of the displacement vector:

$$\delta u_i^* = (u_{im}^* + u_{is}^r C_{sm})\delta p_m^* \tag{3}$$

where C_{sm} are arbitrary constants, δp_m^* are parameters of arbitrary virtual forces, with m indicating the location and direction of application of these forces, $\delta\sigma_{ijm}^*$ and δu_{im}^* are functions with global support of coordinates and directions of δp_m^*, referred as source point (m), and the coordinates and directions where the effects of δp_m^* are measured, referred as field point (i).

The formulation of the consistent boundary element method is developed by considering an approximation of the term b, in equation 2, when knowing a particular solution [1] and through algebraic manipulations it is possible to find the consistent equation of the method,

$$\mathrm{H}(\mathrm{d} - \mathrm{d}^{\mathrm{p}}) = G_a(\mathrm{t} - \mathrm{t}^{\mathrm{p}}) \equiv \mathrm{G}\mathrm{P}_{\mathrm{R}}^{\perp}(\mathrm{t} - \mathrm{t}^{\mathrm{P}}) \tag{4}$$

where $\mathrm{P}_{\mathrm{R}}^{\perp}$ is the orthogonal projector onto the admissible space of surface forces. This equation uses the Somigliana identity, which is based on a system contour data to calculate displacements at internal points.

In Dumont's work [1, 2], it is shown that the interpolation functions present in the formulation are generally polynomials of the natural coordinates of the contour, which works well for the displacements and for the calculation of the matrix H. However, it would not be possible for surface forces to be interpolated by a polynomial along a curved contour, as the forces vary with the inverse of the Jacobian $|J|$, being proposed the replacement of the $t_{i\ell}$ polynomials, referring to the traction forces, by:

$$t_{il} \leftarrow \frac{|J|_\ell}{|J|} t_{i\ell} \tag{5}$$

where $|J|_\ell$ is the value of the Jacobian evaluated at the point ℓ. This format, which is actually part of the proposed consistency improvements, allows for a simpler, accurate execution of the numerical integration of the matrix G.

2.2 Numerical integration of matrices H and G

The fundamental solutions present in the development of the formulation of the boundary element method are determined by the fundamental solutions of Kelvin [5], for the plane state of deformations, indicating expressions for displacements, stresses and surface forces. Thus, matrices H and G can be presented by the following expressions:

$$\mathrm{H} = \frac{-1}{2\pi(1-\nu)}\left\{\int_0^1 \frac{1}{r^2}\mathrm{f}\,\mathrm{d}\xi + \int_0^1 \frac{1}{r^4}\mathrm{h}\,\mathrm{d}\xi\right\} \tag{6}$$

where

$$\mathrm{f} = \left(\frac{1}{2} - \nu\right) N_n^{o_e} \begin{bmatrix} xy' - yx' & xx' + yy' \\ -(xx' + yy') & xy' - yx' \end{bmatrix} \tag{7}$$

$$\mathrm{h} = (xy' - yx')N_n^{o_e} \begin{bmatrix} x^2 & xy \\ xy & y^2 \end{bmatrix} \tag{8}$$

and

$$\mathrm{G} = \frac{-1}{8\pi G(1-\nu)}\left\{\int_0^1 \ln(r)\mathrm{I_g}\,\mathrm{d}\xi + \int_0^1 \frac{1}{r^2}\mathrm{g}\,\mathrm{d}\xi\right\} \tag{9}$$

where

$$\mathrm{I_g} = (3-4\nu)N_\ell^{oe}\begin{bmatrix}1 & 0\\ 0 & 1\end{bmatrix} \tag{10}$$

$$\mathrm{h} = N_\ell^{oe}\begin{bmatrix}x^2 & xy\\ xy & y^2\end{bmatrix} \tag{11}$$

Evaluating the equations, it is possible to identify three types of singularities at different points of an element of the structure [6], illustrated in Fig. 1.

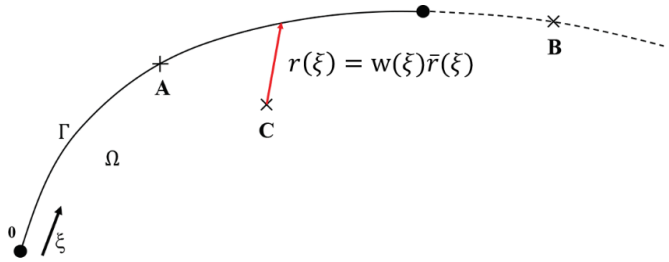

Figure 1. Point locations of singularity, real and complex quasi singularity poles [6]

For a boundary element, using a parametric variable ξ, a singularity can be located at the source point A, within the limits of integration, when 0≤ξ≤1. For the source point B there is a real quasi singularity, located in the element segment, outside the integration limit, but close enough, when ξ>1 or ξ<0. The source point C represents the situation of a complex quasi singularity, positioned outside but close to the integration segment, where ξ=a±bi. These singularities are properly evaluated in the works of Dumont [2, 7].

2.3 Fracture mechanics

The elaboration of this work has important basic concepts of fracture mechanics, resulting from the study of the stress concentration effects produced by Inglis [8] through the analysis of elliptical holes in flat plates, submitted to tensile stresses. The study presented a singularity problem in its formulation: when the radius of curvature of the ellipse tends to zero, the stress value at the extreme point of the ellipse becomes infinite.

Griffith [9] presented a solution to this problem using energy criteria, determining that for a crack propagation to occur, the potential energy Π in the plate, generated by the efforts, must be sufficient to exceed the energy $\mathrm{W_s}$ necessary to break the atomic bonds of the material.

Irwin [10] presented an equivalent energy calculation model to the Griffith model, which consists of measuring the amount of energy available by crack increment, defined as an energy release rate:

$$G = -\frac{d\Pi}{\mathrm{dA}} = \frac{\pi\sigma^2 a}{E} \tag{12}$$

Based on the concept of energy balance presented by Griffith [9], Mai and Lawn [11] presented a study on the crack stability conditions, indicating that the crack stability depends on the second derivative of the system energy, being it greater or less than zero.

$$\frac{\mathrm{d}^2\Pi}{\mathrm{dA}^2} > \frac{\mathrm{d}^2\mathrm{W_s}}{\mathrm{dA}^2} \quad \text{(unstable)} \tag{13}$$

$$\frac{\mathrm{d}^2\Pi}{\mathrm{dA}^2} < \frac{\mathrm{d}^2\mathrm{W_s}}{\mathrm{dA}^2} \quad \text{(stable)} \tag{14}$$

Another important development in fracture mechanics is the stress intensity factor, in which authors such as Westergaard [12], Irwin [13] and Williams [14] developed expressions to calculate stresses in a body subjected to an external load, based on the configuration crack and loading present in the study. There are three loading modes that can act individually, or in combinations of two or three modes simultaneously in a crack [15].

Mode I of loading occurs with a tensile stress, normal to the crack plane. Mode II loading is characterized by in-plane shear of the crack. In this mode, the crack faces slide between each other. The loading mode III, on the other hand, presents shear outside the plane of the crack, performing a "tearing" movement of the plate. All loading modes are illustrated in Fig. 2.

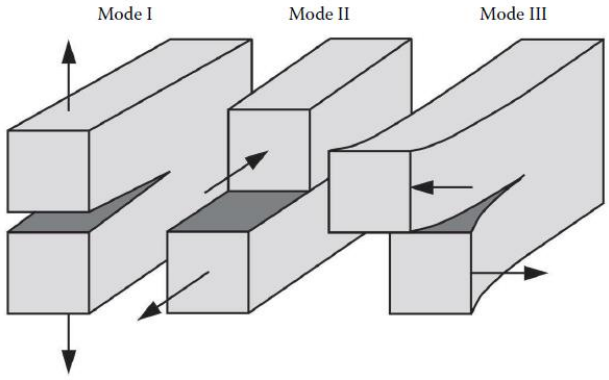

Figure 2. Loading modes on a crack [15, adapted]

In this work, the calculation of the stress intensity factor through the crack tip opening displacement for loading modes I and II will be applied using equations 15 and 16, demonstrated by Dumont and Amaral Neto [6].

$$K_I = \frac{G\sqrt{2\pi}}{4(1-\nu)} \lim_{r\to 0} \frac{\Delta u_{\perp}}{\sqrt{r}} + O(\Delta\theta)^2 \tag{15}$$

$$K_{II} = \frac{G\sqrt{2\pi}}{4(1-\nu)} \lim_{r\to 0} \frac{\Delta u_{=}}{\sqrt{r}} + O(\Delta\theta)^2 \tag{16}$$

where G is the shear modulus of the material, ν is the Poisson ratio, $\Delta u_{\perp}$ and $\Delta u_{=}$ are relative opening and sliding displacements, respectively, between two opposite points on each face, located at the smallest possible distance r from the crack tip and $O(\Delta\theta)^2$ is the error inherent in the model.

In this work, the developments of Westergaard [12] using a complex function, relating the local stress fields to global boundary conditions for certain situations, are also used.

3 Methodology

For this study, two models of two-dimensional plates with edge crack will be considered, illustrated in Fig. 3, in order to initially perform a propagation analysis of only one crack per model. However, it is possible to carry out a propagation analysis in a central elliptical crack, with two or more cracks per model, following the criteria for verifying the occurrence of an extension.

During the design of the models, it was considered that the transverse elastic modulus, G = 80000, Poisson's coefficient, ν = 0.2, the number of Gauss points used in the integration of each element, ng = 4 and a numerical precision of 30 decimal places. The plates have height and width of the same length and are subjected to the same uniform tensile loading applied in the direction of the vertical axis. The first crack model reproduces mode I of loading, while the second model features a loading combination of mode I with mode II.

A problem investigated in this study is the representation of the crack tip shape, considering that the crack faces have a fixed spacing, progressing in parallel to the tip formation. An analysis of the error variation of the stress intensity factor in relation to the relative distance r/a can be performed, compared with results available in the literature. The analysis is performed for quadratic, cubic and quartic boundary elements.

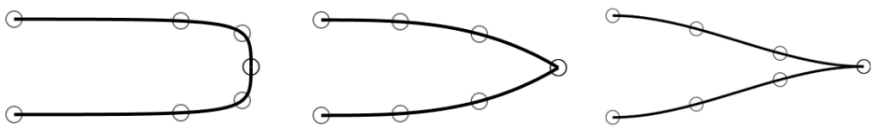

Figure 3. Crack configurations analyzed for cubic elements [16]

For the crack propagation process to occur, it is initially observed whether the material reaches the rupture strength adopted in the study, verified through the stress intensity factor. If it occurs, the propagation direction

angle is calculated. Using the maximum main stress criterion, Lacerda and Wrobel [17] present equation 17, where the angle is calculated with the values of K_I e K_{II}.

$$\alpha = 2\tan^{-1}\left[\frac{1}{4}\left(\frac{K_I}{K_{II}} \pm \sqrt{\frac{K_I}{K_{II}}^2 + 8}\right)\right] \tag{17}$$

The propagation adopted in this study consists of the addition of two elements at the top and bottom faces of the crack, with the same horizontal dimension as the tip element of the crack, Δl. The use of two elements is for a better representation of the propagation process, an angle α with a positive or negative value can be used, and even allows for angles greater than 90º. The crack increment is applied previous to the element belonging to the tip, on both sides, moving the crack tip to a new location, as shown in Fig. 4.

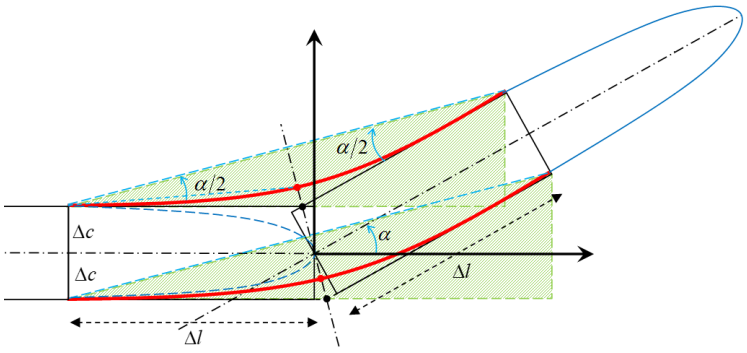

Figure 4. Increment of a propagated crack at an angle α [16]

With the increment of four elements per propagation step, the numbering of the elements and their respective nodes, as well as the data assigned to them, need to be changed. To optimize the execution of the program, only the nodes of the elements at the end of the crack will have their data and connectivity changed, dispensing the reprocessing of most of the data from the matrices used in the program. The elements and nodes added in the increment will follow the numbering of the structure as shown in the local example, illustrated in Fig. 5, of a mesh at the tip of the crack, without changing the order of mesh numbering.

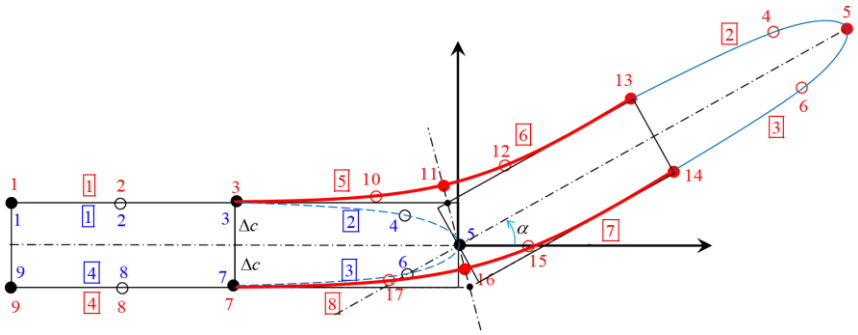

Figure 5. Crack numbering before propagation (blue) and after propagation (red) [16]

After adding the increment, iterative techniques must be used to add new degrees of freedom to the system used in the program.

4 Results

To calculate the stress intensity factor, it was necessary to apply a correction to the displacement data obtained by the program, finding values related to the crack axis, impacting mainly in the case of slanted cracks. Using global coordinates, the following equations were used:

$$U_{\perp} = U_y cos\theta - U_x sen\theta \tag{18}$$

$$U_{=} = U_y sen\theta + U_x cos\theta \tag{19}$$

where $U_{\perp}$ e $U_{=}$ are the opening displacement and the shear displacement of a point with respect to the axis of a crack inclined at an angle θ.

A study was also carried out on the equations regarding the stress intensity factor calculated through the crack tip opening displacement. A model formed by a plate with dimensions 444.5x177.8 was used, containing a crack inclined at 45° with a total length of 177.8/√2, with an origin located at 177.8 from an edge and a uniform tension applied to the smallest face. For the tests, 4 Gauss points were used, transversal elasticity modulus G equal to 80000, Poisson ratio equal to 0.25, quadratic elements and precision of 20 decimal places. The mesh generated by the program is illustrated in Fig. 6.

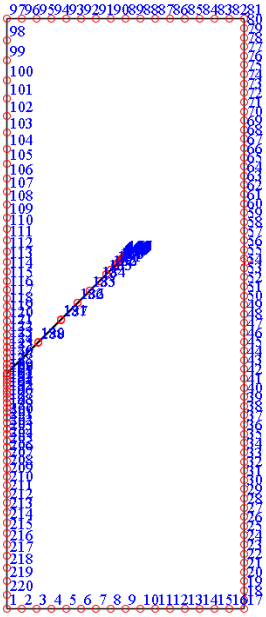

Figure 6. Mesh generated by the program [2], with a more refined discretization at the crack tip

Results of the program were compared with data presented in the literature. The reference values found in the literature for K_I and K_{II} are shown in Table 1, as well as the percentage error of the values found with the program (1.828 for K_I and 0.814 for K_{II}) compared to the values presented by other authors.

Table 1. K_I and K_{II} values and percentage error to literature results

	[18] (Example 1)		[18] (Example 2)		[19]		[20]	
	Value	Error (%)	Value	Error (%)	Value	Error (%)	Value	Error (%)
K_I	1.830	0.109	1.833	0.273	1.778	-2.812	1.856	1.509
K_{II}	0.814	0	0.819	0.611	0.799	-1.877	0.814	2.398

On the crack propagation direction, initially an alternative method was used to verify the maximum stress, by applying internal points at a small distance around the crack tip, positioned in the shape of a semicircle. In the tests, the semicircle is formed by 40 internal points, having a range of 180º, with a radius of 10^{-3}. The greater the proximity of the internal points with the tip of the crack, the greater the errors in the values obtained.

Using the Somigliana identity, already implemented in the program, to find the stress values at the internal points, observing the angle of greatest value and, consequently, the angle of propagation of the crack, with maximum errors in the order of 10^{-4} in relation to the analytical results. This method required a substantial computational effort and was discarded, as only the use of equation 17 was needed to find the final value.

The fracture propagation code, where the process is illustrated in Figures 4 and 5, is currently still being

developed and implemented.

5 Conclusions

In this work, several comparisons with results from the literature were performed to validate the equations implemented in several models, in relation to the stress intensity factor, propagation direction and stability of the structure. Results related to fracture propagation are still in progress.

It is worth noting that the use of the crack tip opening displacement presented considerable errors when the analyzed points were immediately adjacent and far from the crack tip, which could be caused by geometry errors due to mesh refinement and low data accuracy, respectively.

One of the considerations adopted in this study is that, when crack propagation occurs, the faces would keep the same distance from the initial opening, simplifying the iterative process and reducing the computational cost.

Acknowledgements. This project was supported by the Brazilian agencies CAPES and CNPq.

Authorship statement. The authors hereby confirm that they are the sole liable persons responsible for the authorship of this work, and that all material of the present paper is the property (and authorship) of the authors.

References

[1] N. A. Dumont, "The boundary element method revisited". *Boundary Elements and Other Mesh Reduction Methods XXXII*, pp. 227–238, 2010.
[2] N. A. Dumont, "The Collocation Boundary Element Method Revisited: Perfect Code for 2D Problems", *International Journal of Computational Methods and Experimental Measurements*,Vol 6, No. 6, 965-975, 2018.
[3] Maple 15, Maplesoft, a divison of Waterloo Maple Inc. Waterloo, Ontario.
[4] M. H. Aliabadi. *The boundary element method, volume 2: applications in solids and structures*. Vol. 2. John Wiley & Sons, 2002.
[5] Kelvin, Lord. "Note on the integration of the equations of equilibrium of an elastic solid." *Cambridge and Dublin Mathematical Journal,* vol. 3, pp. 87-89, 1848.
[6] N. A. Dumont and O.A. Amaral Neto, "Machine-precise evaluation of stress intensity factors with the consistent boundary element method". *International Journal of Computational Methods and Experimental. Measurements*, vol. 9, n. 2, pp. 141–152, 2020.
[7] N. A. Dumont, "On the eficient numerical evaluation of integrals with complex singularity poles". *Engineering Analysis with Boundary Elements*, vol. 13, n. 2, pp. 155–168, 1994.
[8] C. E. Inglis. "Stress in a plate due to the presence of cracks and sharp corners", *Transactions of the institute of Naval Archtects*, vol. 55, pp. 219-241, 1913.
[9] A. A. Griffth. "The phenomena of rupture and flow in solids", *Philosophical Transactions of the royal society of london. Series A, containing papers of a mathematical or physical character*, vol. 221, n. 582-593, pp. 163-198, 1921.
[10] G. R. Irwin. "Fracture dynamics", *Fracturing of Metals. American Society of Metals*, pp. 296, 1948.
[11] Y. W. Mai and B. R. Lawn, "Crack stability and toughness characteristics in brittle materials". *Annual Review of Materials Science*, vol. 16, n. 1, pp. 415–439, 1986.
[12] H. M. Westergaard, "Bearing Pressures and Cracks: Bearing Pressures Through a Slightly Waved Surface or Through a Nearly Flat Part of a Cylinder, and Related Problems of Cracks.". *Journal of Applied Mechanics*, vol. 6, pp. 49–53, 1939.
[13] G. R. Irwin, "Analysis of stresses and strains near the end of a crack traversing a plate.". *Journal of Applied Mechanics*, vol. 24, pp. 361–364, 1957.
[14] M. L. Williams, "On the stress distribution at the base of a stationary crack.". *Journal of Applied Mechanics*, vol. 24, pp. 109–114, 1957.
[15] T. L. Anderson, *Fracture Mechanics: Fundamental and Applications*. CRC press. New York, 1995.
[16] N. A. Dumont, "*Crack configurations with parallel faces*". Working paper, Pontifical Catholic University of Rio de Janeiro, 2021.
[17] L. A. de Lacerda and L. C. Wrobel, "Dual boundary element method for axisymmetric crack analysis.". *International Journal of Fracture*, vol. 113, n. 3, pp. 267–284, 2002.
[18] R. Namakian, H. M. Shodja and M. Mashayekhi, "Fully enriched weight functions in mesh-free methods for the analysis of linear elastic fracture mechanics problems.". *Engineering Analysis with Boundary Elements*, vol. 43, pp. 1–18, 2014.
[19] X. Zhuang, C. Augarde and S. Bordas, "Accurate fracture modeling using meshless methods, the visibility criterion and level sets: formulation and 2d modeling". *International Journal for Numerical Methods in Engineering*, vol. 86, n. 2, pp. 249–268, 2011.
[20] Y. Murakami, *Stress Intensity Factors Handbook*. Pergamon Press, 1987.